Journal of Nuclear Medicine, published on July 9, 2020 as doi:10.2967/jnumed.120.245597

Ultra-Fast List-Mode Reconstruction of Short PET Frames and Example Applications

Matthew G. Spangler-Bickell[1], Timothy W. Deller[2], Valentino Bettinardi[3], and Floris Jansen[2]

[1]Department of Radiology, University of Wisconsin, Madison, WI, USA. Was with IRCCS Ospedale San Raffaele, Milan, Italy at the time of this study.

[2]PET/MR Engineering, GE Healthcare, Waukesha, WI, USA.

[3]Nuclear Medicine Unit, IRCCS Ospedale San Raffaele, Milan, Italy.

Corresponding:

Matthew Spangler-Bickell

Email: matthew.bickell@gmail.com

Telephone: +1-310-754-5765

ORCID ID: 0000-0003-0465-4004

Manuscript word count: 4963

Disclaimer: Timothy Deller and Floris Jansen are employees of GE Healthcare. Matthew Spangler-Bickell was funded by GE Healthcare at the time of this study. No other potential conflicts of interest relevant to this article exist.

Running title: Ultra-Fast List-Mode Reconstruction

ABSTRACT

Standard clinical reconstructions usually require several minutes to complete, which is mostly independent of the duration of the data being reconstructed. Applications such as data-driven motion estimation which require many short frames over the duration of the scan become unfeasible with such long reconstruction times. In this work we present an infrastructure whereby ultra-fast list-mode reconstructions of very short frames (≤ 1 sec) are performed. With this infrastructure it is possible to have a dynamic series of frames which can be used for various applications, such as data-driven motion estimation, whole-body surveys, quick reconstructions of gated data to select the optimal gate for a given attenuation map, and, if the infrastructure runs simultaneously with the scan, real-time display of the reconstructed data during the scan and automated alerts for patient motion.

Method: A fast ray-tracing TOF projector was implemented and parallelized. The reconstruction parameters were optimized to allow for fast performance: only a few iterations are performed, without point spread function modelling, and scatter correction is not used. The resulting reconstructions are thus not quantitative, but this is acceptable for motion estimation and visualization purposes. Data-driven motion estimation can be performed using image registration, with the resultant motion data being used in a full motion corrected list-mode reconstruction.

Results: The infrastructure is shown to provide images which can be used for visualization and gating purposes, and for motion estimation using image registration. A number of case studies are presented including data-driven motion estimation and correction for brain studies, abdominal studies where respiratory and cardiac motion is visible, and a whole-body survey. Video material is provided in the Supplementary Material.

Conclusion: The presented infrastructure provides the capability to quickly create a series of very short frames for PET data which can be used in a variety of applications.

Keywords: Fast reconstruction, list-mode reconstruction, real-time reconstruction, data-driven motion correction.

INTRODUCTION

Clinical image reconstruction for a single frame of positron emission tomography (PET) data typically requires computation time on the order of minutes. Reconstructions are usually conducted using sinogram data; therefore, the reconstruction time is roughly constant, no matter the acquisition duration or number of coincidence counts in the dataset. Even if reconstruction corrections are disabled and a large pixel size is used, reconstruction computation remains on the order of tens of seconds. This constraint limits potential PET imaging applications. For example, visualization of near real-time images during an ongoing acquisition is made difficult by lengthy reconstruction processing times. Additionally, tracking changes in the activity distribution due to biological processes or patient motion is also impractical. Data-driven motion tracking with high temporal resolution, such as 0.2 sec frames to detect cardiac motion, could require reconstruction processing time approximately 100 times longer than the actual acquisition, even without imaging corrections. This would be computationally prohibitive for a standard clinical protocol.

As a result, data-driven motion detection techniques often avoid the reconstruction step, instead processing on short-duration, coarsely sampled sinogram data. One prominent approach is to apply principal component analysis to these coarse sinograms to detect periodic respiratory motion (*1*). Unfortunately, this approach discards meaningful information in the original dataset, such as the time-of-flight (TOF) dimension. The principal component analysis approach outputs a waveform of motion, but it is not in spatial dimensions. Therefore, it is ineffective for measuring the spatial amplitude of motion, which would allow amplitude-based gating approaches. The time points of non-periodic motion can be detected in short-duration sinogram data, but rigid or nonrigid motion vectors cannot be computed in a reliable way directly from sinogram data.

The multiple acquisition frame technique is an approach that has previously been described to correct for occasional head motion (*2*). As originally described, cameras are used to identify timepoints of motion, and a new frame of sinogram data is started with each motion instance. The multiple frames of data are reconstructed independently, registered to a reference frame, and added together. This approach successfully reduces the motion artifacts, but summing independently reconstructed frames is not a statistically optimal method when using modern iterative reconstruction techniques, and the approach cannot reliably correct slow and extended motion. Preliminary results presented in (*3*) demonstrate a method to estimate the motion parameters directly from the list-mode data, which can then be used in a motion corrected reconstruction. Similarly, in (*4*), centroid-of-distribution calculations estimate when motion occurred followed by frame-wise reconstruction and registration to determine the motion parameters.

In this paper we present an infrastructure to perform very short frame (i.e. ≤ 1 sec) reconstructions faster than the duration of the frame, using list-mode reconstruction. Thus a dynamic series of reconstructed images from very short frames of arbitrary duration is created, and the total time needed to produce the entire series is (1) less than the duration of the data set, and (2) almost constant regardless of the chosen frame duration (although proportional to the total number of coincidence events in the data set, as is typical for list-mode reconstruction).

In the future this infrastructure could be implemented to run simultaneously with the PET acquisition, performing near real-time reconstruction, processing, and visualization of the data. The proposed infrastructure enables many interesting applications. It will be possible to quickly (or in real-time) perform data-driven motion estimation using image registration of the frames, for both rigid and non-rigid applications. Following this estimation a fully motion corrected list-mode reconstruction can be performed. Data-driven gating information can be determined for respiratory and cardiac signals, using either phase-based or amplitude-based approaches. Reconstructed frames can be displayed in near real-time while the patient is in the scanner for the technologist to see, allowing the technologist to verify patient positioning, injection success, observe any patient motion, etc., and to intervene appropriately. Motion can be automatically monitored and an alert triggered for the technologist if motion exceeding a threshold is detected. Quick whole-body surveys can be performed, which could be used, for example, to obtain an overview of areas of interest and adjust the bed durations accordingly to optimize use of the scan time. For gated cardiac imaging, quick reconstructions of gates can be used to select the gate which most closely matches the attenuation map, so that a gated reconstruction can be performed as soon as the acquisition is finished.

The current implementation of the infrastructure operates offline on top of GE Healthcare's (Chicago, IL, USA) standard PET reconstruction research toolbox.

METHOD

Frame Reconstruction

A list-mode reconstruction package was developed as a module which runs on top of the standard research toolbox distributed by GE Healthcare. The list-mode data file is read in short frames which are then reconstructed. The reconstruction has been optimized to produce an image very quickly, faster than the duration of the frame. A future aim is to run this infrastructure online during the data acquisition such that the reconstruction of each short frame would begin as soon as it is finished being acquired, and the reconstruction would be completed and processed before the subsequent short frame is finished acquiring. This would constitute a "near real-time" (one-frame-late) reconstruction and processing of the data.

A fast TOF based ray-tracing projector similar to the Siddon projector (*5*) was implemented. For list-mode reconstruction a TOF projection is faster than non-TOF since only those pixels inside the TOF kernel are visited. In fact, the speed of the projection is proportional to the TOF resolution. The TOF kernels were clipped at ±3 standard deviations. During the projection any event which falls outside of the image field-of-view (FOV) is ignored, and the projection weights for an event are calculated once per iteration and used for both the forward and backprojections. List-mode reconstruction is naturally parallelizable since the projection of each event can be handled independently, with the final backprojected images from each thread being summed. Thus the projector was multi-threaded. To reconstruct each frame pure maximum-likelihood expectation-maximization (MLEM) is used, without subsets, due to the low number of events in each frame. Only $2-5$ iterations are performed, without point spread function modelling. The frame duration can be set arbitrarily, and is usually governed by the activity level and the required task. Durations of 1 second or less are commonly used for most tasks.

For the applications presented here accurate quantitation is not imperative, and therefore no scatter correction is performed. This avoids the computationally expensive step of estimating the scatter contribution. Randoms estimation is calculated from the singles rate on a per-event basis, using the available per-second crystal singles histograms. If desired, attenuation correction is applied using the standard attenuation map generated from either the CT or the MR images. During the initialization of the reconstructions, a sensitivity image is generated and used for all frames.

The following list-mode reconstruction algorithm (*6,7*) is used:

$$\lambda_j^{n+1} = \frac{\lambda_j^n}{\sum_i^I c_{ij} a_i \sigma_i} \sum_m^M c_{i_m j} \frac{1}{\sum_k c_{i_m k} \lambda_k^n + \frac{R_{i_m}}{a_{i_m} \sigma_{i_m}}} \quad (1)$$

where λ_j^n is the image value at pixel j and iteration n, c_{ij} is the system matrix, i_m is the line-of-response (LOR) i associated with list-mode event m, I is the total number of possible LORs in the scanner, M is the total number of list-mode events, a_i is the attenuation correction factor, R_i is the randoms contribution, and σ_i is the scanner sensitivity factor for LOR i.

Image initialization for each frame can be performed in one of two ways: either from a uniform image of ones or using the result of the previous frame after post-smoothing. Using the previous frame can result in visually improved images which are nearer to convergence, and might therefore be appropriate for visualization purposes. However, for motion estimation in the presence of significant motion, this method may introduce bias from one frame to the next. Therefore the appropriate method should be selected based on the task at hand.

Reconstruction Time

A standard Intel i9 CPU laptop computer with 8 cores was used for the benchmarking reported in this section. Using a FOV of 300 mm with pixel dimensions of [2.34, 2.34, 2.78] mm^3, image size [128, 128, 89], and 2 iterations, the typical reconstruction time per frame is given in Table 1 for a number of standard clinical scenarios. Note that the reconstruction time of each frame is consistently less than the frame duration, which is necessary to achieve real-time processing. The reconstruction time of each frame scales approximately linearly with each dimension of the image size (regardless of FOV or pixel size), and linearly with the number of iterations. Certain initialization steps were performed before each run which took ~20 sec. The majority of this initialization time is spent on calculating the sensitivity image, which could be pre-calculated as soon as the attenuation map is ready.

Additionally, a dynamic ^{15}O-H_2O cardiac study was processed to observe the frame reconstruction time as the number of events in each frame varied throughout the scan. A constant frame duration of 0.2 sec was used, and the events per frame and the reconstruction times are shown in Figure 1. The frame reconstruction time scales approximately linearly with the number of events in the frame. The deviation from linearity during the early frames just after the injection is due to a large number of random events in those frames, many of which do not pass through the image FOV leading to a faster than normal reconstruction time. As can be seen in Figure 1, for frames with more than 900×10^3 events the reconstruction time could surpass the frame duration. This is easily solved by limiting the number of events used for the reconstruction of those frames. This was not necessary in any of the cases presented in this paper.

This linear relationship implies that for a given data set, the total time taken to reconstruct all frames is approximately constant regardless of the chosen frame duration, except for a small but non-zero overhead contribution.

Data-Driven Motion Correction

The dynamic series of short frames can be used to estimate the motion by performing image registration between each frame and a chosen reference frame. For brain scan data rigid registration is performed, which can be started as soon as a frame reconstruction is complete. A mean-square difference metric is used with a gradient-descent optimizer. Attenuation correction is not applied to avoid possible bias introduced by a mismatch between the PET data and attenuation map in the presence of motion. Initial tests indicate that both the frame reconstruction and registration can be performed faster than real-time. Therefore it is possible to fully estimate the motion concurrently with the scan, such that as soon as the acquisition is completed a fully motion-corrected list-mode reconstruction can be performed, as is presented in (*8*).

It was reported in (*9*) that a rigid registration with an accuracy (defined as the average error after registration in the brain position, which is calculated using multiple points scattered throughout the brain) of approximately 1 mm can be achieved for FDG brain scan data on frames containing approximately 40×10^3 true coincidence counts. For standard scans this frame count level corresponds to a frame duration of about 0.26 seconds. While such a short frame duration will translate to a high temporal resolution of the motion estimates, it is perhaps excessive in most cases and a frame duration of 1 second should provide adequate motion sampling while allowing for more robust image registration.

APPLICATIONS

Informed consent was received for all studies in accordance with the institutions' review boards.

Real-Time Reconstruction

Brain Study: A dementia patient underwent an ^{18}F-FDG brain study in the 20 cm axial FOV configuration Discovery-MI PET/CT scanner (GE Healthcare) at UZ Leuven, Belgium. During the scan the patient moved their hand into the FOV and scratched their forehead. This was not evident until the data was reconstructed into short frames using the methodology presented above. The data was reconstructed into 1 second frames and each frame contained approximately 400×10^3 list-mode events. Two MLEM iterations were performed using pixel dimensions of [3.26, 3.26, 2.78] mm^3 and a FOV of 300 mm, a uniform image was used for the initialization, and post-smoothing with a full width at half maximum (FWHM) of 8 mm was applied. Each frame was reconstructed in 0.2 sec. A time range in which the patient's hand can be seen entering the FOV is available in Supplemental Video 1 (supplemental materials are available at http://jnm.snmjournals.org), and a selection of representative frames is shown in Figure 2.

Abdominal Studies: In Figure 3 are shown multiple examples of reconstructed frames over the abdomen from standard clinical scans on the SIGNA PET/MR (GE Healthcare) at Ospedale San Raffaele (OSR), Milan, Italy. All of the studies used pixel dimensions of [2.34, 2.34, 2.78] mm^3, a FOV of 300 mm, 2 iterations, and 14 mm FWHM isotropic post-smoothing. The frames were of duration 0.1 - 0.3 sec, contained 50-100 $\times 10^3$ events, and were reconstructed faster than real-time. Figure 3(A) is a ^{68}Ga-DOTATOC study and shows respiratory motion of the abdominal organs. Figure 3(B) is an FDG study showing the bed position over the heart, and the cardiac motion can be seen. Finally Figure 3(C) is another FDG study where the transport of the urine from the kidneys into the bladder can be seen. Videos of these frames can be seen in Supplementary Videos 2 - 4. Such images could be displayed in near real-time for the technologist to see, but could also be used for non-rigid motion correction, for data-driven gating, or for selecting the appropriate gate to match the attenuation map from the CT.

Data-Driven Motion Correction

Case I: A clinical FDG brain study was conducted on the SIGNA PET/MR scanner at OSR. During the scan the patient spoke to the technologist causing significant motion of their head, and the head did not return to the initial position. The movement of the patient's jaw was visible in the short reconstructed frames, as can be seen in Figure 4 as well as in Supplementary Video 5. Reconstructions were performed of 1 sec frames containing ~400×10^3 events using pixel dimensions of [2.34, 2.34, 2.78] mm^3, a FOV of 300 mm, 2 iterations, and 8 mm FWHM isotropic post-smoothing, and the motion of the head was estimated using image registration. The plots of the 6 degrees-of-freedom are shown in Figure 5. Had the technologist been alerted that the patient's head did not return to its initial position they could possibly have taken appropriate measures (such as restarting the scan). Nonetheless, with these motion estimates a full motion corrected list-mode reconstruction was performed, the result of which is shown in Figure 5, using pixel dimensions [1.17, 1.17, 2.78] mm^3, FOV 300 mm, 3 iterations with 47 subsets, with point spread function modelling, and 4 mm FWHM post-smoothing.

Case II: A 20 minute clinical ^{11}C-methionine study was conducted on the SIGNA PET/MR scanner at OSR. In the last 5 minutes of the scan the patient moved their head to the one side and then the other. This motion was estimated using the described methodology with 2 sec frames containing ~600×10^3 events, and the estimated motion was used to perform a full motion corrected reconstruction with pixel dimensions [1.17, 1.17, 2.78] mm^3, a FOV of 300 mm, using 5 iterations with 28 subsets, with point spread function modelling, and with a 4 mm FWHM post-smoothing. The result of this reconstruction is shown in Figure 6.

Whole-Body Survey

To perform a rapid whole body survey a patient could be moved through the scanner in less than 5 seconds (the limiting factor being the maximum bed speed and patient comfort), and the data quickly reconstructed. Such data could be used to identify areas of interest and thereby guide how the subsequent scan time is divided amongst the bed positions.

A standard whole body data set from a patient undergoing an FDG scan on the SIGNA PET/MR at OSR was used to visualize what such a survey might look like. A single frame of duration 0.3 seconds from each of 5 bed positions was reconstructed, containing 50-100 $\times 10^3$ events, and the frames were stitched together. Each frame was reconstructed using 2 MLEM iterations, with pixel dimensions [2.34, 2.34, 2.78] mm^3, and with a 14 mm FWHM post-smoothing filter. The maximum intensity projection of the resulting reconstruction is shown in Figure 7. This image is comprised of only 1.5 seconds of data which demonstrates how quickly the whole-body survey could be acquired. A video of multiple consecutive frames from this study can be seen in Supplementary Video 6.

DISCUSSION

The presented methodology allows for ultra-fast reconstruction, processing, and/or visualization of acquired PET data producing a dynamic series of images with very short frame durations. The fast reconstructions are achieved by using an optimized time-of-flight ray-tracing projector within a multithreaded CPU setting, and using efficient reconstruction parameters such as only 2 - 5 MLEM iterations and no scatter correction. If this infrastructure were to be used on the scanner during acquisition then the applications presented in this report here could be performed in near real-time. As demonstrated, such an infrastructure enables, for example, fast and automatic data-driven motion estimation using image registration, real-time visualization of the tracer distribution for the technologist to see, quick whole-body surveys, and quick reconstructions of gated data to select the optimal gate given the attenuation map. We expect that once this infrastructure is available to users and researchers other applications will be developed which take advantage of the dynamic series of short-frame reconstructed images.

Scanner capabilities play a role in the image quality and usefulness of short-duration PET frames. A large PET detector axial field of view provides additional anatomical coverage for input to registration algorithms. Timing resolution has been previously demonstrated to improve edge definition (*10,11*) and provide robustness (*12*) when attenuation correction is not applied. Detector sensitivity provides a signal- to-noise benefit that allows for shorter frames and therefore improved temporal resolution. The scanners employed in this study were the GE SIGNA PET/MR (*13*) and the 4-ring GE Discovery MI (*14*). Both of these scanners utilize modern silicon photomultipliers (*15*) and have favorable specifications among clinical PET systems in each of these categories.

For rigid motion estimation, the methodology presented here uses fully reconstructed images and image registration to estimate the motion faster than the real-time of the data, with a temporal resolution ($\geq$ 1 Hz) which is sufficient for almost any possible patient head motion. A full list-mode event-by-event motion correction can then be performed using these estimated motion parameters, as in (*8*). This could be applied retrospectively to any list-mode data set. Estimating the motion directly using reconstructed images results in the actual 6 degrees-of-freedom of the motion parameters rather than indicators of when motion occurred.

The cardiac and respiratory motion can be tracked and quantified, for gating purposes or for non-rigid motion estimation. Deformation parameters could be estimated from the short frames and used in a motion corrected reconstruction. This will be further investigated in the near future. Whether this motion estimation could be performed faster than real-time will need to be evaluated.

The current implementation results in non-quantitative reconstructions since scatter is not corrected for. While this is not imperative for the applications which we have demonstrated, there are applications, such as kinetic modelling, for which this would be important. Additionally, the reconstructions are not iterated until convergence, thus we intend to investigate other algorithms which converge faster than MLEM. Lastly, for data-driven motion estimation using image registration, if the tracer dynamics cause a significant change in the distribution during the acquisition then the registration to the chosen reference frame may fail. Methods to handle such situations will be implemented.

CONCLUSION

An infrastructure to perform ultra-fast reconstructions of very short frames of list-mode data has been presented. Sub-second frames can be reconstructed faster than real-time. The resulting series of reconstructions can be used for various applications, such as data-driven motion estimation. Once this infrastructure is made available online during the PET data acquisition, the near real-time frames could be displayed for the technologist to see during the scan. Other possible applications have been demonstrated here for various clinical case studies for brain, abdomen, and whole body scans.

DISCLOSURE

Timothy Deller and Floris Jansen are employees of GE Healthcare. Matthew Spangler-Bickell was funded by GE Healthcare at the time of this study. No other potential conflicts of interest relevant to this article exist.

ACKNOWLEDGMENTS

The authors gratefully acknowledge Prof. Dr. K. Van Laere of UZ Leuven, Belgium, and Uppsala University Hospital, Sweden, for providing clinical data, Mohammad Mehdi Khalighi of Stanford University, Palo Alto, CA, USA, for assistance with data, and Charlotte Hoo of GE Healthcare, Chicago, IL, USA, for acceleration contributions to the software.

KEY POINTS

QUESTION: What applications become possible if ultra-fast reconstructions of very short PET data frames are available?

PERTINENT FINDINGS: An infrastructure for reconstructing very short frames (≤ 1 sec) of list-mode PET data faster than the frame duration is presented. Examples applications are demonstrated of real-time visualization of the PET data during acquisition, data-driven image-based motion estimation, and quick whole body surveys.

IMPLICATIONS FOR PATIENT CARE: This work implies many significant clinical implications: improved patient monitoring using the real-time tracer distribution, improved diagnostic value of images through motion estimation and correction, optimized use of scan time by taking whole body surveys, etc.

REFERENCES

1. Thielemans K, Schleyer P, Dunn J, Marsden PK, Manjeshwar RM. Using PCA to detect head motion from PET list mode data. *IEEE Nucl Sci Symp Conf Rec*. 2013:1–5.
2. Picard Y, Thompson C. Motion correction of PET images using multiple acquisition frames. *IEEE Trans Med Imaging*. 1997;16:137-44.
3. Feng T, Yang D, Zhu W, Dong Y, Li H. Real-time data-driven rigid motion detection and correction for brain scan with listmode PET. *IEEE Nucl Sci Symp Conf Rec.* 2016;1-4.
4. Lu Y, Naganawa M, Toyonaga T, et al. Data-driven motion detection and event-by-event correction for brain PET: Comparison with Vicra. *J Nucl Med*. January 31, 2020. [Epub ahead of print].
5. Siddon RL. Fast calculation of the exact radiological path for a three-dimensional CT array. *Med Phys*. 1985;12:252-255.
6. Reader AJ, Erlandsson K, Flower MA, Ott RJ. Fast accurate iterative reconstruction for low-statistics positron volume imaging. *Phys Med Biol*. 1998;43:835.
7. Parra L, Barrett HH. List-mode likelihood: EM algorithm and image quality estimation demonstrated on 2-D PET. *IEEE Trans Med Imaging*. 1998;17:228–235.
8. Spangler-Bickell MG, Khalighi MM, Hoo C, et al. Rigid motion correction for brain PET/MR imaging using optical tracking. *IEEE Trans Radiat Plasma Med Sci*. 2018;3:498–503.
9. Spangler-Bickell MG, Deller T, Hurley SA, McMillan AB, Bettinardi V, Jansen F. Effect of image noise on registration in PET brain imaging. *IEEE Nucl Sci Symp Conf Rec*. 2019:1-3.
10. Wollenweber SD, Ambwani S, Lonn AHR, et al. Comparison of 4-class and continuous fat/water methods for whole-body, MR-based PET attenuation correction. *IEEE Trans Nucl Sci*. 2013;60:3391–3398.
11. Qian H, Manjeshwar RM, Ambwani S, Wollenweber SD. Truncation completion of MR-based PET attenuation maps using time-of-flight non-attenuation-corrected PET images. *IEEE Nucl Sci Symp Conf Rec*. 2012:2773–2775.
12. Conti M. Why is TOF PET reconstruction a more robust method in the presence of inconsistent data? *Phys Med Biol*. 2010;56:155.
13. Grant AM, Deller TW, Khalighi MM, Maramraju SH, Delso G, Levin CS. NEMA NU 2-2012 performance studies for the SiPM-based TOF-PET component of the GE SIGNA PET/MR system. *Med Phys*. 2016;43:2334–2343.

14. Hsu DFC, Ilan E, Peterson WT, Uribe J, Lubberink M, Levin CS. Studies of a next-generation silicon-photomultiplier-based time-of-flight PET/CT system. *J Nucl Med*. 2017;58:1511- 1518.
15. Levin CS, Maramraju SH, Khalighi MM, Deller TW, Delso G, Jansen F. Design features and mutual compatibility studies of the time-of-flight PET capable GE SIGNA PET/MR system. *IEEE Trans Med Imaging*. 2016;35:1907–1914.

Scan type	Scanner	Tracer	Injected activity (MBq)	Time P.I. (min)	Events per frame	Frame duration (sec)	Frame recon time (sec)
Brain	D-MI	^{18}F-FDG	231	80	400×10^3	1.0	0.18
Cardiac	SIGNA	^{18}F-FDG	259	143	55×10^3	0.1	0.07
Abdomen	SIGNA	^{68}Ga-DOTATOC	137	121	60×10^3	0.3	0.07

TABLE 1. Frame-based execution times for various clinical scenarios using a standard 8-core Intel i9 CPU system. Note that the initialization of each run took ~20 sec.

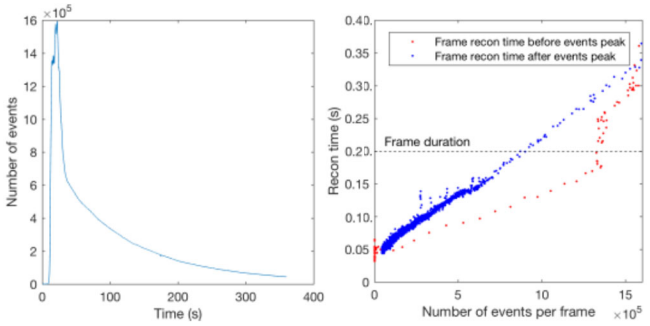

FIGURE 1. (Left) A plot of the events per 0.2 sec frame recorded during a dynamic ^{15}O-H_2O cardiac study. (Right) A plot illustrating the linear relationship between the reconstruction time per frame and the number of events in the frame. The dashed line indicates the real duration of the frames. The red points are for those frames before the peak in the events per frame. These frames occur immediately after the injection and contain a high fraction of random events which do not pass through the image FOV, leading to faster than normal reconstruction times. Note that for frames with a high number of events ($> 9 \times 10^5$) the reconstruction times were longer than the frame durations. Data courtesy of Uppsala University Hospital.

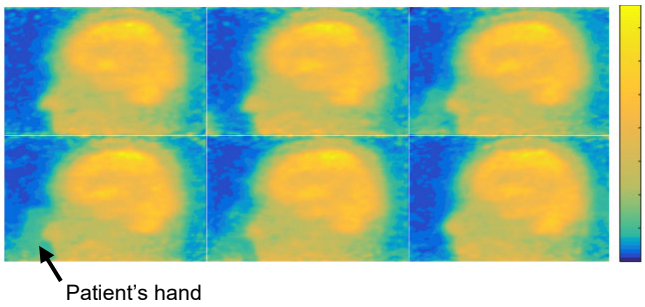

FIGURE 2. From top left to bottom right: Reconstructions of consecutive 1 second frames. The patient's hand can be seen inside the FOV in the middle four frames. Note that the color scale has been adjusted to highlight the patient's hand. Data courtesy of UZ Leuven (Prof. Dr. K. Van Laere). A corresponding video of these frames is shown in Supplementary Video 1.

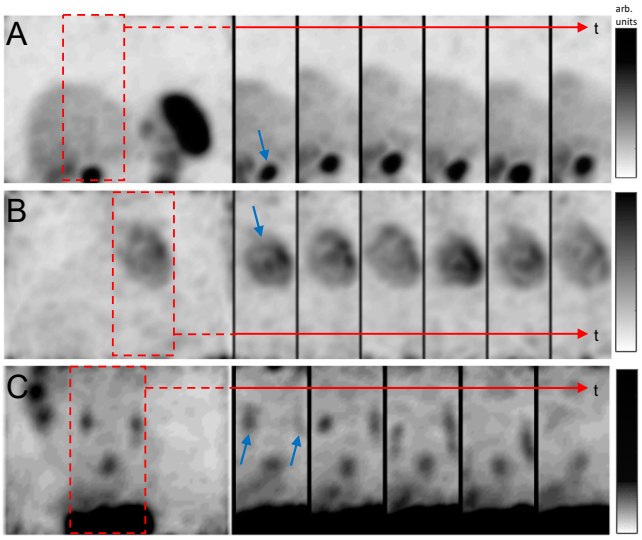

FIGURE 3. (A) Maximum intensity projections (MIPs) of frames from a clinical ^{68}Ga-DOTATOC abdominal study. Several consecutive frames are shown where the motion due to respiration can be observed. The frames are of duration 0.3 sec. The red arrow indicates the time axis. (B) MIPs of several frames over the heart from a clinical FDG study, where the cardiac motion can be observed. The frame durations were 0.1 sec. (C) MIPs of several frames over the abdomen from a clinical FDG study where the transporting of the urine into the bladder can be seen. The frame durations were 0.3 sec. Corresponding videos of these frames are shown in Supplementary Videos 2-4.

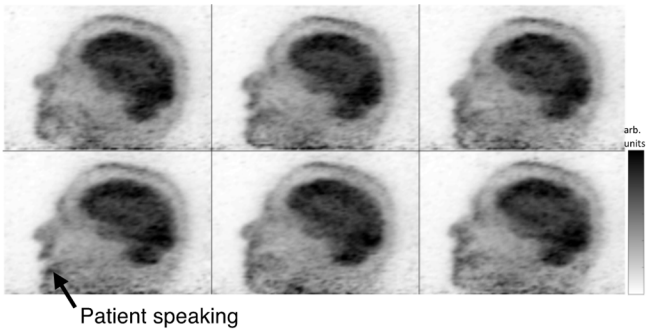

FIGURE 4. Selected frames of 1 sec duration from top left to bottom right where the patient can be seen speaking during the scan. A corresponding video of these frames is shown in Supplementary Video 5.

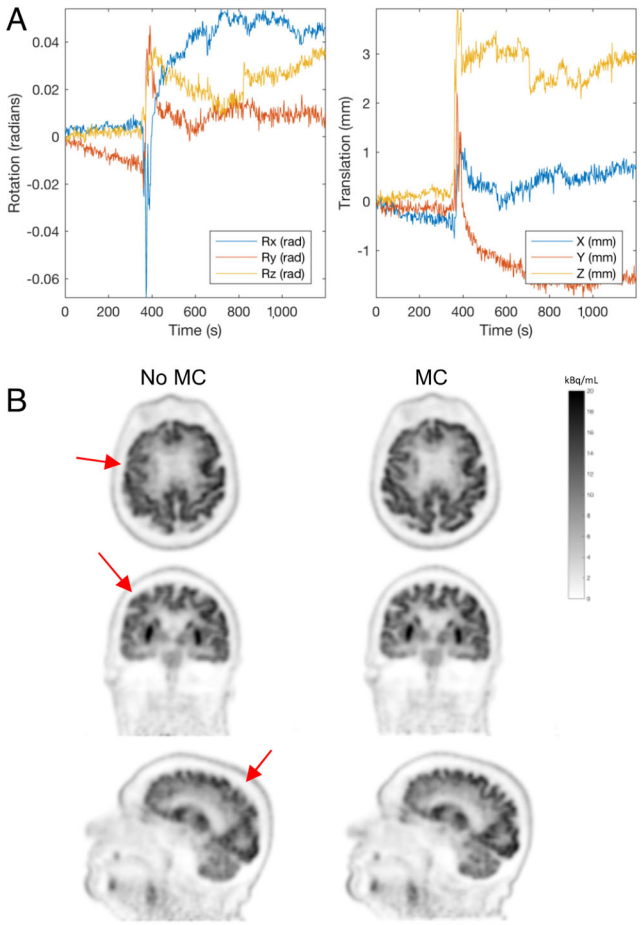

FIGURE 5. (A) Plots showing the 6 degrees-of-freedom of the estimated motion for the patient's head. The patient spoke at about 380 sec, and the head did not return to its initial position following the motion. (B) A list-mode reconstruction without (left) and with (right) motion correction (MC). The red arrows indicate where motion blurring can be observed, which has been removed in the motion corrected reconstruction.

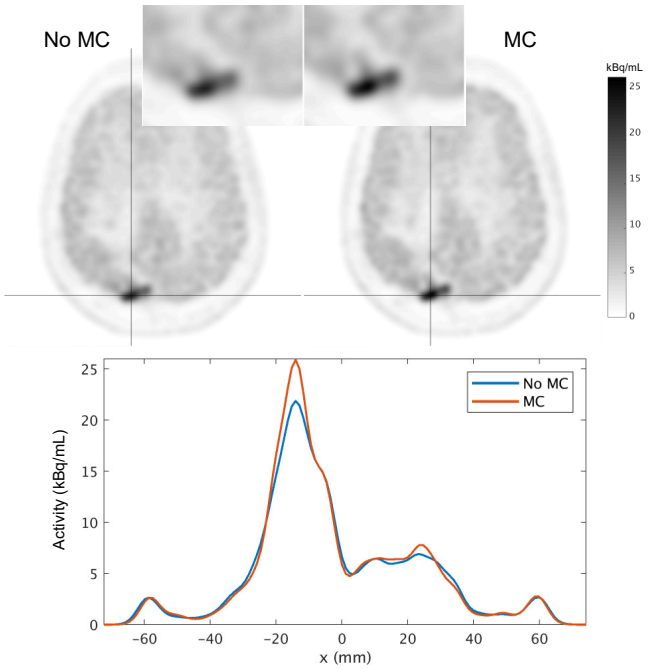

FIGURE 6. A methionine study where the patient moved their head during the scan. Slight loss of resolution of the lesion can be seen in the zoomed in inset in the non-motion corrected image (top left). The profiles through the lesion (along the horizontal black line) indicate a clear quantitative difference when applying motion correction.

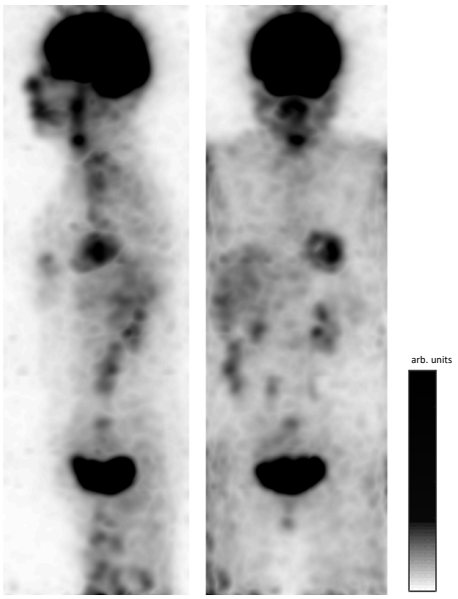

FIGURE 7. Sagittal and coronal maximum intensity projections of single frames from 5 beds of an FDG study stitched together. Each frame was of duration 0.3 seconds and thus this image is comprised of 1.5 seconds of data in total. A corresponding video of these frames is shown in Supplementary Video 6.

Supplemental files attached to PDF